A Letters Journal Exploring the Frontiers of Physics

January 2008

EPL, **81** (2008) 10009
doi: 10.1209/0295-5075/81/10009

www.epljournal.org

Breaking chirality in nonequilibrium systems on the lattice

Diego Pazó[1] and Ernesto M. Nicola[2]

[1] *Instituto de Física de Cantabria, IFCA (CSIC-UC) - Avda. Los Castros, 39005 Santander, Spain*
[2] *Max-Planck-Institut für Physik komplexer Systeme - Nöthnitzer Straße 38, 01187 Dresden, Germany*

received 1 August 2007; accepted in final form 3 November 2007
published online 3 December 2007

PACS 05.45.-a – Nonlinear dynamics and chaos
PACS 47.54.-r – Pattern selection; pattern formation
PACS 02.30.Oz – Bifurcation theory

Abstract – We study the dynamics of fronts in parametrically forced oscillating lattices. Using as a prototypical example the discrete Ginzburg-Landau equation, we show that much information about front bifurcations can be extracted by projecting onto a cylindrical phase space. Starting from a normal form that describes the nonequilibrium Ising-Bloch bifurcation in the continuum and using symmetry arguments, we derive a simple dynamical system that captures the dynamics of fronts in the lattice. We can expect our approach to be extended to other pattern-forming problems on lattices.

Extended systems on lattices have played a major role in the development of nonlinear science. One may recall celebrated models as the discrete sine-Gordon equation or the Fermi-Pasta-Ulam experiment. Usually, the development of the field has been associated with conservative systems, but dissipative lattices have attracted growing attention in the last two decades (see [1] for a review). Two prominent examples of such lattices are provided by the discrete version of the Nagumo and Ginzburg-Landau partial differential equations. The former has been proposed as a model of myelination of neuronal fibres [2]; and the latter describes, among others, dissipative solitons [3], the dynamics of lines of vortices [4] and coupled wakes [5] in hydrodynamics.

The complex Ginzburg-Landau equation [6] universally describes the dynamics of an extended medium in the neighbourhood of an oscillatory instability. Under homogeneous resonant $n:1$ forcing, different regions of space may lock to the driving with different phase relations; and domain walls separate these regions. The prototypical $2:1$ resonant case leads to the so-called parametrically forced complex Ginzburg-Landau (FCGL) equation. This equation has been the subject of extensive study since the seminal work by Coullet and coworkers in ref. [7]. There it was found a front bifurcation which is the nonequilibrium analogue of the Ising-Bloch transition in ferromagnets.

In this letter, we show that the dynamics of fronts in the FCGL equation *on the lattice* is captured by a normal form consisting of two ordinary differential equations. The bifurcations linking different dynamics of the front (including bistable regimes) are observed both in a projection of the system's variables onto a cylindrical phase space and in the normal form. Our results are relevant for experiments where discretisation is given as in arrays of coupled pendula [8,9], electronic circuits [10,11], or chemical systems [12]; and also in systems usually modeled as continuous, but that are intrinsically discrete (or behave like a lattice due to a spatially periodic modulation of the medium).

For a lattice, the FCGL equation [13,14] takes the form

$$\dot{A}_j = (1+i\nu)A_j - (1+i\beta)|A_j|^2 A_j + \gamma A_j^* + \kappa(1+i\alpha)(A_{j+1}+A_{j-1}-2A_j)\,, \tag{1}$$

where $A_j \equiv \rho_j e^{i\psi_j}$ is a complex variable. The parameter γ measures the forcing strength, and κ controls the coupling between neighboring units. Parameters ν, β, and α account for the detuning, the nonisochronicity, and the dispersion, respectively.

The continuum limit. – First of all, we recall the results for the continuous version of (1):

$$\partial_t A = (1+i\nu)A - (1+i\beta)|A|^2 A + \gamma A^* + (1+i\alpha)\Delta A\,. \tag{2}$$

Vanishing values of ν, β, and α allow to cast (2) into a variational form: $\partial A/\partial t = -\delta\mathcal{F}/\delta A^*$. In this case, stable front solutions minimise the energy functional $\mathcal{F}$, and depending on the forcing γ they can be chiral ($\gamma < \gamma_{IB} = 1/3$) or achiral ($\gamma \geqslant \gamma_{IB}$). If A vanishes at the centre of the front the so-called *Ising* front is found, otherwise the

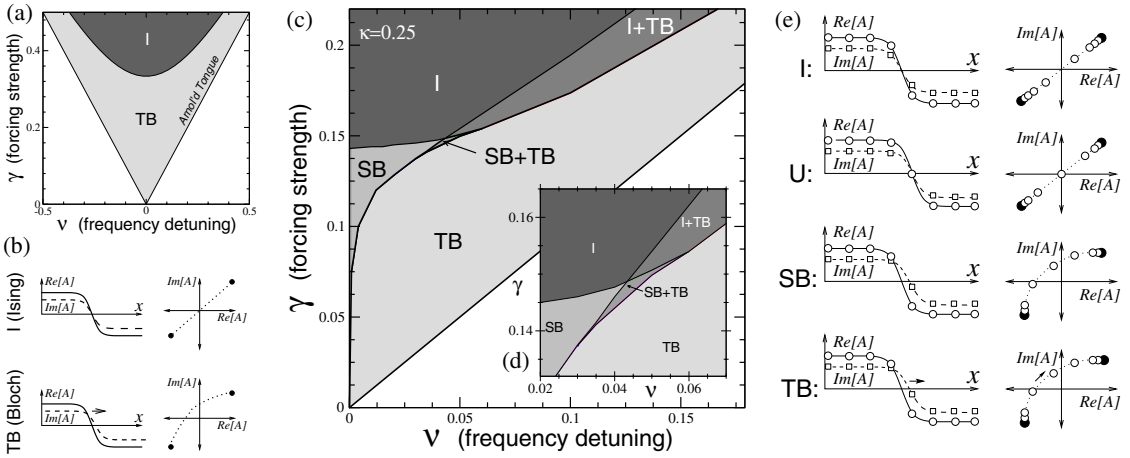

Fig. 1: Regions in the parameter space ν-γ where Ising (I) and travelling or stationary Bloch fronts (denoted by TB and SB, respectively) appear: (a) in the continuum, and (c) on the lattice, $\kappa = 0.25$ in eq. (1). Sketches of all possible fronts (b) in the continuum, and (e) on the lattice. Whereas the fronts I, TB and SB in (e) are stable for some parameter values, the front U is always unstable.

front is chiral and A does not vanish anywhere: two such *Bloch* solutions with opposite chirality exist.

The nonequilibrium Ising-Bloch (NIB) transition is observed for nonzero values of ν, β, or α [7,15]. The terms ν, β and α are perturbations to a gradient system, and cause the Bloch fronts to move, in either direction depending on their chirality (see [14] and references therein).

Front dynamics. – We restrict ourselves hereafter to the case $\beta = \alpha = 0$, so that ν remains as the parameter that breaks the variational character of the system; we note nevertheless that the same qualitative results are obtained perturbing variationality through ν, β, and α. Inside the region $\gamma > |\nu|$ (the *Arnold tongue*), see fig. 1(a), the local dynamics is bistable with two stable fixed points $A_{S\pm} = \pm\rho_S e^{i\psi_S}$ with $\rho_S = [1+\sqrt{\gamma^2-\nu^2}]^{1/2}$, and $\psi_S \in (-\pi/2, \pi/2)$ the solution of $\sin(2\psi_S) = \nu/\gamma$, $\cos(2\psi_S) = (\rho_S^2 - 1)/\gamma$. The fixed point at the origin $A_O = (0,0)$ is either completely unstable ($\gamma^2 < 1+\nu^2$), or saddle ($\gamma^2 > 1+\nu^2$). We are interested in the dynamics of fronts connecting the two stable fixed points: $A_{j\to\mp\infty} = A_{S\pm}$.

In the continuum, the locus of the NIB transition can be calculated analytically [16]: $\gamma_{NIB}(\nu) = [\sqrt{1+9\nu^2}]/3$, see fig. 1(a) (and fig. 1(b) for a sketch of both front types). As mentioned above, for $\nu = 0$ we recover the variational case, $\gamma_{NIB}(\nu = 0) = \gamma_{IB}$, and Bloch fronts are stationary.

Our extensive numerical simulations of the FCGL equation on the lattice[1] have revealed several front types not present in the continuum. These fronts are sketched in fig. 1(e) and figs. 1(c), (d) show their regions of stability. Stationary Bloch fronts (SB) exist on a finite region of parameter space around an interval of the line $\nu = 0$. Additionally, two regions of bistability are found: In one of them Ising and travelling Bloch fronts coexist (I+TB). The other bistable region (SB+TB) is shown in fig. 1(d), and it is a small triangle with stable stationary and travelling Bloch fronts.

Cylindrical coordinates. – A projection of the $2N$ degrees of freedom onto a two-dimensional phase space greatly simplifies the analysis of the fronts. One way of performing this projection is

$$\Phi = \mathrm{Re}\left[\sum_{j=1}^{N} \frac{\rho_j}{\rho_S} e^{i(\psi_j - \psi_S)}\right], \tag{3}$$

$$C = \mathrm{Im}\left[\sum_{j=1}^{N} \frac{\rho_j}{\rho_S} e^{i(\psi_j - \psi_S)}\right]. \tag{4}$$

This corresponds to a rotation and compression of the complex plane A such that the stable fixed points are now located on the real axis at ± 1. This projection permits us to discern if a front is symmetric with respect to the origin (in such a case $C = 0$). Note that Φ is a cyclic variable that takes the same value when the front advances or recedes one lattice unit (provided the front is far from the boundaries) and thus can be defined modulo 2. The variable C measures the deviation from stationarity and is intrinsically bounded.

Typical examples of the dynamics in the reduced coordinates (3)-(4) are shown in figs. 2(a), (b). Two stationary fronts, both with $C = 0$, exist for all parameter values. One, the Ising front (I), is located at $(\Phi, C) = (0,0)$ if the number of units N is even (or at $(1,0)$ if N is odd) and is a continuation for $\kappa > 0$ of the trivial solution at zero coupling: $[\ldots, A_{S+}, A_{S+}, A_{S+}, A_{S-}, A_{S-}, A_{S-}, \ldots]$. The second stationary solution, denoted U, is at $(1,0)$ (respectively, at $(0,0)$ for odd N), and is a continuation of the unstable front solution: $[\ldots, A_{S+}, A_{S+}, A_O, A_{S-}, A_{S-}, \ldots]$.

[1] The numerical calculations were performed with zero flow boundary conditions $A_0 = A_1$, $A_{N+1} = A_N$, and a lattice size N large enough to neglect boundary effects on the front dynamics (with N typically being 128).

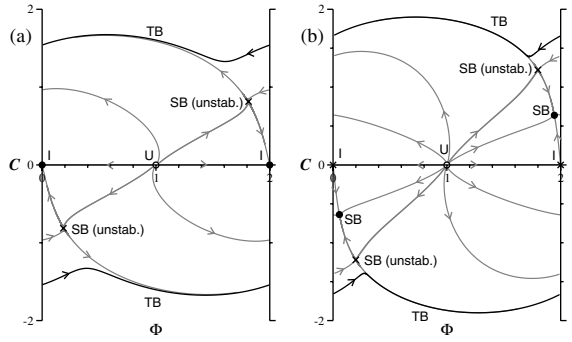

Fig. 2: Numerically obtained flows projecting the front dynamics onto the cylindrical phase space Φ-C defined by eqs. (3) and (4). In (a) an example of coexistence I+TB is shown ($\nu = 0.1$ and $\gamma = 0.183$). In (b) SB+TB ($\nu = 0.045$ and $\gamma = 0.148$). Symbols $\bullet, \times, \circ$ denote stable, saddle and unstable fixed points, respectively.

For some parameter values, there exist extra fixed points located off the Φ-axis. We label these chiral solutions stationary Bloch (SB) fronts. Travelling Bloch (TB) fronts correspond to periodic orbits around the cylinder. Due to symmetry they always appear in pairs circulating in opposite directions.

Normal form. – Next, we present a simple ordinary-differential-equation model that generates dynamics like the front dynamics on the FCGL lattice. We will obtain this normal form via symmetry arguments.

In continuous systems the NIB transition is a parity-breaking (pitchfork) bifurcation coupled to a translation-invariant coordinate. It is an example of the so-called drift-pitchfork bifurcation found in a number of situations (*e.g.* [17]), usually as a secondary instability. Its normal form is [18,19] $\dot{\phi} = c$, $\dot{c} = (\mu - c^2)c$, where μ is the bifurcation parameter, *e.g.*, $\mu \propto (\gamma_{NIB} - \gamma)$. Coordinates ϕ, c represent the position and the velocity of the concerned structure (the front in our case).

Knobloch *et al.* [20] considered the breakdown of the *continuous* translational invariance to study the parity breaking of a periodic pattern in the presence of an inhomogeneity. This leads to the inclusion of small periodic terms (sinusoidals in the simplest case) that preserve the invariance under inversion $(\phi, c) \to (-\phi, -c)$:

$$\dot{\phi} = c - \epsilon \sin\phi\,, \tag{5}$$

$$\dot{c} = (\mu + \delta\cos\phi - c^2)c + \eta\sin\phi\,, \tag{6}$$

where ϕ is now an angular variable. In [21] it was suggested that this normal form could also be used to analyse parity-breaking bifurcations found in discrete bistable media (*e.g.*, arrays of FitzHugh-Nagumo units).

In the continuum, as the variational limit is approached the velocity of the Bloch front decreases (and becomes zero at variationality). Consequently, we introduce a small parameter χ that accounts for the deviation from the variational case. For the situation considered here, χ is proportional to[2] ν. We have then at leading order:

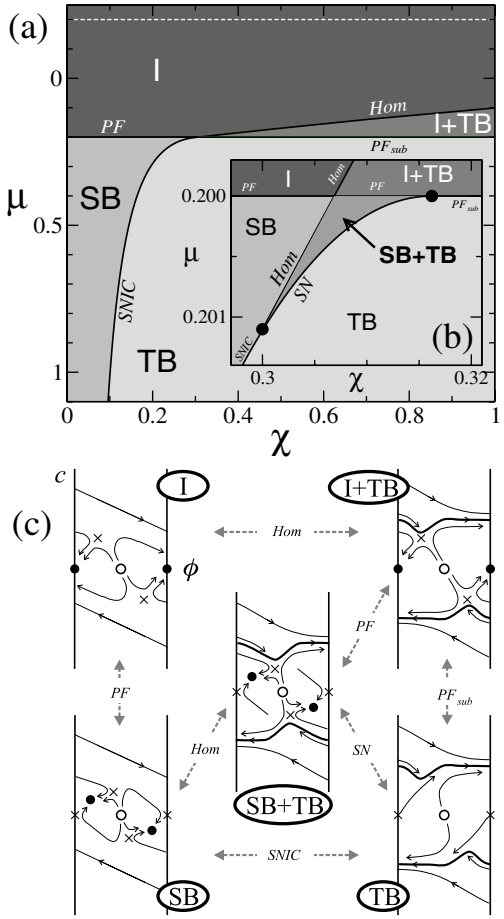

Fig. 3: (a), (b) Parameter space of the normal form (7)-(8) with $\epsilon = 0.1$ and $\delta = -0.2$; the loci of local and global bifurcations are depicted with solid lines. The black dots in the inset (b) indicate the location of two codimension-2 bifurcation points. (c) Schematic representation of the phase space ϕ-c for the five regions in (a), (b). Gray-dashed lines indicate the link between different states via codimension-1 bifurcations (PF and PF_{sub} are, respectively, super- and sub-critical pitchfork, and *SN*, *Hom*, and *SNIC* stand for (off-cycle) saddle-node, homoclinic, and saddle-node on an invariant circle bifurcations).

$$\dot{\phi} = \chi c - \epsilon\sin\phi\,, \tag{7}$$

$$\dot{c} = (\mu + \delta\cos\phi - c^2)c. \tag{8}$$

The term $\eta\sin\phi$ present in (6) is absent in (8) due to the invariance of the discrete FCGL equation under the transformation $(\nu, \beta, \alpha, A) \to (-\nu, -\beta, -\alpha, A^*)$. This requires the symmetry under $(\chi, \phi, c) \to (-\chi, \phi, -c)$ to be satisfied. This considerably simplifies the normal form.

Figure 3(a) shows the regions of the parameter space χ-μ, and fig. 3(c) is a sketch of the corresponding phase spaces. The normal form (7)-(8) qualitatively reproduces

[2] According to eq. (4) in [7], in the variational limit one has $\chi \propto \nu - \beta - (\alpha - \beta)\gamma$.

front dynamics, which can indeed be projected on a cylinder, *e.g.* the phase space Φ-C introduced above. There are two pitchfork bifurcations at $\mu = \pm\delta$ and the parameter space is organised by two codimension-2 points. We may see in fig. 3(b) that at a degenerate pitchfork point located at $\hat{\chi}^2 = -2\epsilon^2/\delta$ the pitchfork bifurcation line switches between subcritical and supercritical. The second codimension-2 point is a saddle-node separatrix-loop point [22] where the saddle-node bifurcation on the invariant circle (*SNIC*) splits into an off-cycle saddle-node (*SN*) and a homoclinic (*Hom*) bifurcation.

In contrast to the continuous case, travelling Bloch fronts appear with nonzero chirality, and the (average) velocity of the front v asymptotically follows: i) the familiar square-root law when crossing the *SNIC* line; ii) a logarithmic law below the homoclinic line: $v^{-1} = a - (1/\lambda_u)\ln(\gamma - \gamma_{Hom})$, where λ_u is the positive eigenvalue corresponding to the saddle Bloch front.

Let us finally discuss the parameters modelling the discretisation strength: ϵ and δ. In the continuum limit, our numerical simulations indicate that discretisation enters in the normal form through δ at order $O(\kappa^{-1})$, whereas ϵ vanishes much faster (possibly exponentially) as $\kappa \to \infty$. In addition, assuming opposite signs for ϵ and δ correctly inherits the bifurcations in the anticontinuum limit ($\kappa \to 0$). Accordingly, our choice $\epsilon = 0.1$ and $\delta = -0.2$ in fig. 3(a) satisfies these constraints (*i.e.* $|\epsilon| < |\delta|$, $\epsilon\delta < 0$). The organisation of the parameter space is qualitatively robust to changes of both parameters in a wide range.

Phase equation. – The normal form (7), (8) is obtained in a perturbative way including small terms that model the breakdown of translational invariance, and the departure from $(\nu, \beta, \alpha; \gamma) = (\mathbf{0}; \gamma_{IB})$, the equilibrium Ising-Bloch bifurcation point. This means that we cannot predict the behaviour of the bifurcation lines far from this point. In particular, the (*SNIC*) bifurcation line, which separates SB and TB regions in fig. 1(c), can be proved to end at $\nu = \gamma = 0$ as results from the following facts. For small γ, a phase reduction [7,14] of the FCGL lattice yields a discrete Nagumo-type equation (the overdamped Frenkel-Kontorova (FK) model): $\dot{\psi}_j = \nu - \gamma\sin(2\psi_j) + \kappa(\psi_{j+1} + \psi_{j-1} - 2\psi_j)$. Interestingly, ν acts as a symmetry-breaking parameter, but the symmetry of the original model is hidden in the factor 2 inside the $\sin(2\psi_j)$ term, which allows two mirror front solutions connecting $\psi_{j\to-\infty} = \psi_S$ and $\psi_{j\to\infty} = \psi_S + \pi$. Discreteness implies the existence of an interval of "propagation failure" [2] where propagation is blocked for nonvanishing ν. Well-established results for the FK model (see, *e.g.*, [23,24]) state that the propagation threshold (*SNIC* line) should approach the γ-axis exponentially fast[3] as $\gamma \to 0$.

Conclusions. – The nonequilibrium Ising-Bloch bifurcation in the parametrically driven complex Ginzburg-Landau equation is one of the most studied pattern instabilities. In the continuum, breaking of chirality causes the front to move. However, as shown here, on the lattice a more complex scenario appears: specifically, two types of bistability and a region with chiral (Bloch) stationary fronts. We have demonstrated that a normal form with two variables captures the dynamics of the front and the bifurcations between different regions. It is to be emphasised that the normal form (7)-(8) is based on symmetry arguments that provide general qualitative results independent of details as, for instance, the parameter of nonvariationality or the discretisation order of the Laplacian.

The dynamics of patterns on lattices is typically much harder to solve analytically than in their continuous counterparts. The continuum, usually serves as a zeroth-order approximation that is not necessarily accurate. Discreteness typically introduces new dynamical regimes as shown in the current letter for one spatial dimension[4]. Through a modification of the normal form for the continuum, we have been able to reproduce the dynamics of fronts on a discrete medium and the structure of parameter space. This approach should also work in other problems on lattices.

* * *

We thank M. A. Matías, J. M. López, E. Montbrió and L. G. Morelli for useful discussions and critical comments. DP acknowledges support by *Ministerio de Educación y Cultura* (Spain) through the Juan de la Cierva Programme. This work was supported by MEC (Spain) under Grant No. FIS2006-12253-C06-04.

REFERENCES

[1] Scott A., *Nonlinear Science: Emergence of Dynamics and Coherent Structures* (Oxford University Press, Oxford) 1999.

[2] Keener J. and Sneyd J., *Mathematical Physiology* (Springer-Verlag, New York) 1998.

[3] Akhmediev N. and Ankiewicz A. (Editors), *Dissipative Solitons, Lect. Notes Phys.*, Vol. **661** (Springer, Berlin) 2005.

[4] Willaime H., Cardoso O. and Tabeling P., *Eur. J. Mech. B*, **10** (1991) 165; Cardoso O., Willaime H. and Tabeling P., *Phys. Rev. Lett.*, **65** (1990) 1869.

[5] Gal P. L., *C. R. Acad. Sci. Paris*, **313** (1991) 1499; Ravoux J. F., Dizès S. L. and Gal P. L., *Phys. Rev. E*, **61** (2000) 390.

[6] Aranson I. S. and Kramer L., *Rev. Mod. Phys.*, **74** (2002) 99.

[3] Recent results for a different nonlinearity suggest, however, that the threshold vanishes at particular values ("pinning failure") what would imply that the *SNIC* line touches the γ-axis at some values, and possibly a singular behaviour in the $\gamma \to 0$ limit; see [25] for details.

[4] In two dimensions an even higher number of dynamical regimes can be expected to appear due to discreteness, since the continuous FCGL equation already exhibits a variety of patterns such as spirals, labyrinths, stripes, hexagons, etc. (see, *e.g.*, [26]). Discreteness should give rise to a plethora of exotic patterns, such as spiral waves with extended defects [27].

[7] Coullet P., Lega J., Houchmanzadeh B. and Lajzerowicz J., *Phys. Rev. Lett.*, **65** (1990) 1352.
[8] Denardo B., Galvin B., Greenfield A., Larraza A., Putterman S. and Wright W., *Phys. Rev. Lett.*, **68** (1992) 1730.
[9] Huang G., Lou S. Y. and Velarde M. G., *Int. J. Bifurcat. Chaos*, **6** (1996) 1775.
[10] Bode M., Reuter A., Schmeling R. and Purwins H.-G., *Phys. Lett. A*, **185** (1994) 70.
[11] Pérez-Muñuzuri V., Pérez-Villar V. and Chua L. O., *Int. J. Bifurcat. Chaos*, **2** (1992) 403.
[12] Laplante J. P. and Erneux T., *J. Phys. Chem.*, **96** (1992) 4931.
[13] Walgraef D., *Spatio-Temporal Pattern Formation, with Examples in Physics, Chemistry and Materials Science* (Springer Verlag, New York) 1996.
[14] Mikhailov A. S. and Showalter K., *Phys. Rep.*, **425** (2006) 79.
[15] Barra F., Descalzi O. and Tirapegui E., *Phys. Lett. A*, **221** (1996) 193.
[16] Skryabin D. V., Yulin A., Michaelis D., Firth W. J., Oppo G.-L., Peschel U. and Lederer F., *Phys. Rev. E*, **64** (2001) 056618.
[17] Gollub J. P. and Meyer C. W., *Physica D*, **6** (1983) 337; Migler K. B. and Meyer R. B., *Phys. Rev. Lett.*, **66** (1991) 1485; Nasuno S., Yoshimo N. and Kai S., *Phys. Rev. E*, **51** (1995) 1598; Pan L. and de Bruyn J. R., *Phys. Rev. E*, **49** (1994) 483; Brunet P., Flesselles J.-M. and Limat L., *Europhys. Lett.*, **56** (2001) 221; Liehr A. W., Bödeker H. U., Röttger M. C., Frank T. D., Friedrich R. and Purwins H.-G., *New J. Phys.*, **5** (2003) 89; Marts B., Hagberg A., Meron E. and Lin A. L., *Phys. Rev. Lett.*, **93** (2004) 108305; Thiele U., John K. and Bär M., *Phys. Rev. Lett.*, **93** (2004) 027802; Leonetti M., Nuebler J. and Homble F., *Phys. Rev. Lett.*, **96** (2006) 218101.
[18] Dangelmayr G. and Knobloch E., *Philos. Trans. R. Soc. London, Ser. A*, **322** (1987) 243.
[19] Kness M., Tuckerman L. S. and Barkley D., *Phys. Rev. A*, **46** (1992) 5054.
[20] Knobloch E., Hettel J. and Dangelmayr G., *Phys. Rev. Lett.*, **74** (1995) 4839; Dangelmayr G., Hettel J. and Knobloch E., *Nonlinearity*, **10** (1997) 1093.
[21] Pazó D., Deza R. R. and Pérez-Muñuzuri V., *Phys. Lett. A*, **340** (2005) 132.
[22] Schecter S., *SIAM J. Math. Anal.*, **18** (1987) 1142.
[23] Kladko K., Mitkov I. and Bishop A. R., *Phys. Rev. Lett.*, **84** (2000) 4505.
[24] Carpio A. and Bonilla L. L., *SIAM J. Appl. Math.*, **63** (2003) 1056.
[25] Elmer C. E., *Physica D*, **218** (2006) 11.
[26] Coullet P. and Emilsson K., *Physica D*, **61** (1992) 119.
[27] Izús G., Pazó D., Deza R. R. and Pérez-Muñuzuri V., *Phys. Rev. E*, **72** (2005) 045205.